REFERENCES

1. P.J. Nussbaum, S.D. Tayabji, and A.T. Ciolko. Prestressed Pavement Joint Designs. FHWA, June 1981.
2. S.D. Tayabji, B.E. Colley, and P.J. Nussbaum. Prestressed Pavement Thickness Design. FHWA, June 1981.
3. B.F. Friberg. Prestressed Pavements--Theory into Practice. Proc., International Conference on Concrete Pavement Design, Purdue Univ., West Lafayette, IN, 1977.
4. J.H. Emanual and J.L. Hulsey. Prediction of the Thermal Coefficient of Expansion of Concrete. Journal of the American Concrete Institute, April 1977.
5. Design and Control of Concrete Mixtures. Portland Cement Association, Skokie, IL, 1979.
6. T.C. Hansen and A.H. Mattock. Influence of Size and Shape of Member on the Shrinkage and Creep of Concrete. Journal of the American Concrete Institute, Vol. 63, No. 2, Feb. 1966.
7. P.J. Nussbaum, B.F. Friberg, A.T. Ciolko, and S.D. Tayabji. Prestressed Pavement Construction Manual. FHWA, June 1981.
8. A.N. Hanna, P.J. Nussbaum, T. Arriyavat, J. Tseng, and B.F. Friberg; Portland Cement Association. Technological Review of Prestressed Pavements. FHWA, Rept. FHWA-RD-77-8, Dec. 1976.
9. L.W. Teller and E.C. Sutherland. The Structural Design of Concrete Pavements. Public Roads, Vol. 23, No. 8, April-June 1943, pp. 167-212.
10. B.F. Friberg. Investigations of Prestressed Concrete Pavements. HRB, Bull. 332, 1962, pp. 40-94.
11. E.F. Kelley. Structural Design of Concrete Pavements. Journal of the American Concrete Institute, Vol. 35, Supplement, Sept. 1939.
12. G.R. Morris and H.C. Emery. The Design and Construction of Arizona's Prestressed Concrete Pavement. Research Section, Highway Division, Arizona Department of Transportation, Phoenix, Jan. 1978.
13. G.E. Albritton. Prestressed Concrete Highway Pavement: Performance During Construction. Paper presented at 57th Annual Meeting, Transportation Research Board, Washington, DC, Jan. 1978.

Publication of this paper sponsored by Committee on Rigid Pavement Design.

Prestressed Pavement Thickness Design

S.D. TAYABJI, B.E. COLLEY, AND P.J. NUSSBAUM

A computerized procedure for thickness design of zero-maintenance prestressed concrete pavements is presented. Factors considered in developing the design procedure include traffic loading, temperature and moisture variation in the concrete slab, loss of subbase support, properties of concrete, properties of subbase, properties of subgrade, and effective midslab prestress. The procedure is based on flexural stress analysis and prevention of bottom transverse cracking that may initiate from the longitudinal edge of the slab in the vicinity of midslab. Inputs for the computer program include number and magnitude of axle loadings, wheel placement, traffic volume distribution during a 24-h day, temperature data, load transfer effectiveness, and effective prestress at midslab. Program output is in terms of total fatigue consumption at the end of design life. If fatigue consumption is less than 100 percent, then the thickness meets design criteria. A design example is presented for a rural four-lane highway in Illinois.

The objective of the Federal Highway Administration (FHWA) Research Project 5E, Premium Pavements for Zero Maintenance, is to exploit modern materials and technology in developing zero-maintenance pavements for warranted use. As a portion of this research project, an investigation has been conducted by Construction Technology Laboratories, a division of the Portland Cement Association. The objective of the investigation was to develop design and construction techniques for prestressed concrete pavements.

Conventional concrete pavements are designed on the basis of concrete's relatively low modulus of rupture without effectively using the natural advantage of its high compressive strength. In prestressed pavements, precompression in the concrete due to prestressing increases allowable stress in the flexural zone. Precompression causes the reduction or elimination of cracking and a large decrease in the number of transverse joints. Consequently, a more comfortable riding surface is provided and maintenance costs are reduced.

Prestressed pavement design includes the determination of required pavement thickness and joint hardware. Joint hardware is determined based on anticipated slab movement and length. Figure 1 shows the basic steps involved in prestressed pavement design.

As shown in Figure 1, the design process is iterative and involves the interaction of many factors. The process starts with the selection of an initial slab thickness. Then, for joint hardware design, trial main slab length and prestress tendon size, spacing, and force are selected. Effective midslab prestress is computed. A minimum of about 50-psi midslab prestress should be obtained. If it is not obtained, slab length, tendon size, spacing, or force is varied until the desired midslab prestress is obtained. A minimum prestress is desirable to ensure that the early shrinkage cracks that may develop remain tightly closed. Thus, load transfer across possible cracks is improved due to aggregate interlock.

When the midslab prestress criterion is satisfied, anticipated maximum joint movement is computed. Selection of an appropriate joint infiltration-prevention device such as a strip seal, compression seal, or steel cover plate depends on the magnitude of total joint movement. Total movement may be accommodated at one or two active joints between adjacent slabs. Slab length is varied until the computed joint movement can be accommodated by the device selected.

After slab length, midslab prestress level, and joint hardware are established, a structural analysis is performed. This analysis requires the value

Figure 2. Tandem axle load configuration.

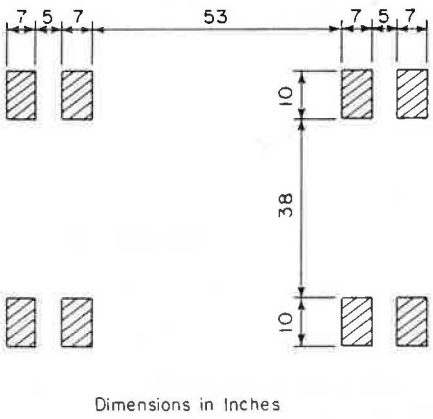

Figure 3. Load placement coefficients, C_e.

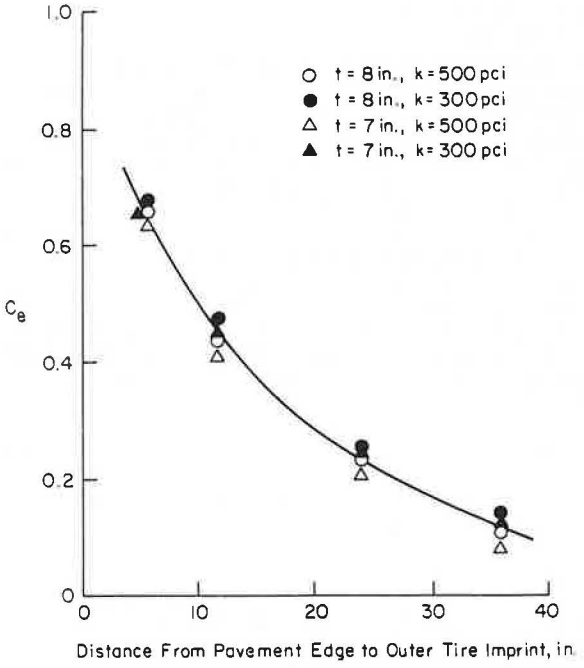

Traffic Load Stresses

A finite-element computer program for analysis of slabs on a Winkler (liquid) foundation was used to compute moments for the case of edge loading (2). These moments, expressed as a function of the radius of relative stiffness (1), are stored in this computer program. They are used together with a coefficient to determine edge stresses that result from loads located at or inward from the pavement edge. The program also considers optional use of a tied concrete shoulder with a variable input for load-transfer efficiency at the longitudinal joint.

Either a single- or a tandem-axle load configuration may be selected as input. Wheel imprint dimensions and wheel and axle spacings used in the program are shown in Figure 2. For single-axle loading, the wheel imprint size and spacings are the same.

Moments at the pavement edge due to loads at the edge are given by the following equations. For an 18-kip single-axle load,

$$M = 483.4(l)^{0.571} \text{ in-lb} \quad (1)$$

where M is the bending moment at edge, and l is the radius of relative stiffness of pavement (in), i.e.,

$$l = \sqrt[4]{Eh^3/[12(1-u^2)k]} \quad (2)$$

where

E = modulus of elasticity of concrete (psi),
h = slab thickness (in),
u = Poisson's ratio = 0.15, and
k = modulus of subgrade reaction (psi).

For a 36-kip tandem-axle load,

$$M = 185.1(l)^{0.820} \text{ in-lb} \quad (3)$$

Moment equations are based on the assumption of loss of subbase support for a 20-in distance inward from the pavement edge. This adjustment is made to recognize upward slab warping due to moisture differentials in the pavement.

Load stress (f_L) is determined by the following equation:

$$f_L = (6M/h^2)(P/18\,000\,n)\,C_e \text{ psi} \quad (4)$$

where

P = single- or tandem-axle load (lb),
n = 1 for single-axle load and 2 for tandem-axle load, and
C_e = load placement coefficient.

The load placement coefficients shown in Figure 3 are provided as program input. These coefficients are used to reduce stress at the pavement edge when loads are applied in wheel paths located inward from the edge.

Equation 4 for load stress (f_L) can be further modified to incorporate the contribution of a tied shoulder. This is done by using the following equation:

$$f_L = (6M/h^2)(P/18\,000\,n)C_e[1/(1+JE)] \text{ psi} \quad (4a)$$

where JE is joint efficiency, i.e., JE = deflection at shoulder side of joint divided by deflection at main pavement side of joint.

Traffic Characteristics

Axle loads and lateral placement of loads across the pavement during different periods of a 24-h day are program inputs. Curling stresses vary during the day, and maximum curling stresses exist for only short durations of time. Therefore, the traffic distribution during the entire day is required to equate maximum stresses to the number of load applications during selected time periods. Time periods and traffic during the selected periods are program inputs.

States accumulate traffic loadometer data in the format used in FHWA W4 loadometer tables. These tables tabulate the number of axles observed within load groups and are generally reported for 2000-lb increments. For concrete pavements, traffic projections are made for design periods that usually range from 20 to 40 years.

A recommended lateral distribution of traffic is shown in the table below:

Distance from Outside Wheel to Pavement Edge (in)	Truck Traffic (%)
0-6	20
6-12	20
12-18	25
18-24	15
24-30	10
30-36	5

These values were selected based on information obtained by Emery (3). Traffic volume is subdivided with respect to time of day. A recommended distribution is given in the user's manual.

Temperature Effects

Curling stresses develop in a slab when temperatures vary with depth. During daytime when the top surface is warmer than the bottom, tensile stresses develop at the slab bottom. During nighttime when temperature gradients are reversed, tensile stresses develop at the slab top. For stress calculations, it is generally assumed that the temperature gradient is linear. The maximum gradient is assumed to be about 3°F/in during daytime and about 1°F/in during nighttime. In practice, the temperature distribution is usually nonlinear and constantly changing. Also, maximum daytime and nighttime temperature differentials exist for short time durations.

Because the daily variation of air temperature follows an approximately sinusoidal cycle, temperature variations at the slab surface can be assumed to be sinusoidal. This variation can be represented as follows (4,5):

$$\theta_T = \theta_o \sin(2\pi t/T) \quad (5)$$

where

θ_T = temperature at surface of slab,
θ_o = constant = amplitude of the temperature cycle at slab surface,
t = time of day (24-h clock), and
T = 24 h.

Equation 5 represents daytime conditions well but gives an incorrect distribution for nighttime conditions. For nighttime, the amplitude is about one-third of that computed by using this equation. Therefore, for nighttime conditions, θ_o is replaced by θ_o' which is equal to $\theta_o/3$. Accuracy of the nighttime temperature distribution is not as critical because these stresses are subtracted from the load stresses.

For homogeneous semi-infinite solids whose surface temperature varies sinusoidally, the temperature (θ_z) at any time t on a plane at depth z below the surface is given by

$$\theta_z = \theta_o \exp(-\beta) \cdot \sin[(2\pi t/T) - \beta] \quad (6)$$

where

$\beta = (z/\psi^2)\sqrt{\pi/T}$,
ψ^2 = diffusivity of the material (in^2/h) = $\lambda/\gamma c$,
λ = thermal conductivity of the material (Btu/h-ft-°F),
γ = weight per unit volume of the material (lb/ft), and
c = specific heat of the material (Btu/lb-°F).

For a concrete slab resting on earth or subbase, Equation 6 is applicable, as diffusivities of the materials are similar. For concrete,

λ = 1.20 Btu/h-ft-°F,
γ = 145 lb/ft^3,
c = 0.22 Btu/lb-°F, and
ψ^2 = 542 in^2/h.

By using this procedure, calculated variations in temperature distribution with time for concrete pavement thicknesses of as much as 10 in are shown in Figure 4. These data are more representative of measured field data than the assumption of a linear temperature distribution. For example, temperature distributions shown in Figure 4 agree well with those measured at the American Association of State Highway Officials (AASHO) Road Test (6).

Average slab temperature (θ_M) at time t is obtained by integrating Equation 6 for θ_z between 0 and the slab thickness (H) and dividing by H. The difference (θ_D) between average slab temperature and slab bottom temperature (θ_B) is given by

$$\theta_D = \theta_M - \theta_B \quad (7)$$

Curling stress at the bottom of the edge of a long slab is given by

$$f_c = \alpha E \theta_D \quad (8)$$

where α is the coefficient of thermal expansion. This nonlinear temperature distribution formulation is used in the computerized design procedure to calculate curling stresses.

Its use requires an input value for θ_o shown in Equation 5. For U.S. conditions, a recommended value is 30°F; however, other values may be substituted where local information is available and conditions are substantially different.

Moisture Effects

Top-to-bottom variations in pavement moisture con-

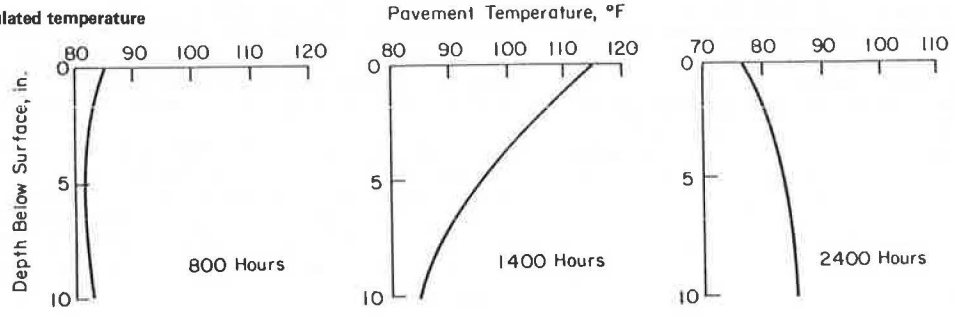

Figure 4. Calculated temperature distribution.

tent result in bottom fiber compressive stresses. Ideally, these stresses would be calculated for cyclical seasonal changes in moisture content. Calculated stresses would then be used in the thickness design procedure in the same manner as temperature stresses. However, only limited data are available regarding top-to-bottom moisture distribution, seasonal moisture variation, or stress magnitude.

Friberg (7) and Nagataki (8) report that restrained warping strain at the slab bottom may be about 150 millionths. These data are valuable and serve to direct future research. However, it is assumed currently that warping stresses for 7- and 8-in-thick pavements are 190 and 220 psi, respectively.

Warping also results in loss of support along the pavement edge. Loss of support causes an increase in edge stress associated with traffic loading. Effects of upward warping on load stress calculations are included in Equations 1 and 3.

Subbase Support

Pavement performance is related to the quality of subbase and subgrade support. Ideally, as shown in Figure 1, a thickness design procedure should incorporate allowable subbase and subgrade deformations as limiting criteria. For a concrete pavement in contact with the subbase at a corner or edge, these deformations could be related to slab deflection. However, measured concrete pavement deflections are influenced by temperature and moisture gradients in the concrete at the time of testing. Therefore, sufficient data are not available to develop criteria for correlating subbase and subgrade deformations with pavement deflection.

For given load conditions, prestressed concrete pavements are thinner than conventional concrete pavements. Thus, subbase support requirements are more critical. For zero-maintenance projects, it is recommended that a high-quality subbase be used with prestressed pavements. Modulus of subgrade reaction at the top of the subbase should be about 500 lb/in³.

Fatigue of Concrete

Flexural fatigue research on concrete has shown that as the ratio of flexural stress to modulus of rupture decreases, the number of stress repetitions to failure increases (9). Allowable load repetitions for stress ratios between 0.50 and 0.85 are given by the following equation (10):

$$\log(NN) = 11.83 - 12.20(f_T/MR) \quad (9)$$

where

NN = allowable stress repetitions,
f_T = total flexural stress, and
MR = concrete modulus of rupture (psi).

The above equation is used in the program. However, at the designer's option, other fatigue equations may be used as program input.

Midslab Prestress

Midslab prestress is computed by accounting for prestress losses due to tendon friction, concrete shrinkage, concrete creep, steel relaxation, and subbase friction restraint. A minimum of about 50-psi midslab prestress should be available. This is achieved by properly selecting slab length and tendon force, size, and spacing. Selection is an iterative process. Several trial calculations are generally required before the desired value of midslab prestress is obtained. Details of midslab prestress computation are given in the following discussion.

Tendon Friction

Tendon friction results from curvature and wobble. Curvature is due to intentional and wobble to unintentional tendon profile variations. Tendon friction (f_t) is determined from the following equation:

$$f_t = f_{pe}\left(1 - \exp\left\{-[ux + (KL/2)]\right\}\right) \text{ psi} \quad (10)$$

where

f_{pe} = end prestress (psi),
u = curvature friction coefficient,
x = angular change of tendon from jacking end to midslab (radians),
K = wobble friction coefficient per foot, and
L = slab length (ft).

For straight portions of pavements, intentional angular changes are negligible. Therefore, tendon friction can be obtained from the following equation:

$$f_t = f_{pe}\left\{1 - \exp[-(KL/2)]\right\} \text{ psi} \quad (11)$$

Concrete Shrinkage

Prestress loss due to concrete shrinkage (f_s) is given by the following equation:

$$f_s = \epsilon_s E_s (A_s/A_c) \text{ psi} \quad (12)$$

where

ϵ_s = concrete shrinkage strain,
E_s = modulus of elasticity of tendon steel (psi),
A_s = area of tendon per unit width of slab (in²), and
A_c = area of slab per unit width of slab (in²).

Concrete Creep

Prestress loss due to concrete creep (f_{cr}) is given by the following equation:

$$f_{cr} = C_u(E_s/E_c)f_{pe}(A_s/A_c) \text{ psi} \quad (13)$$

where C_u is the ultimate creep coefficient and E_c is the modulus of elasticity of concrete (psi).

Steel Relaxation

Prestress loss due to steel relaxation (f_r) is given by the following equation:

$$f_r = \rho f_{pe} \text{ psi} \quad (14)$$

where ρ is the relaxation coefficient for the appropriate stress level.

Subbase Friction

Prestress loss due to subbase friction (f_f) is given by the following equation:

$$f_f = [(U_s \gamma^L)/288] \text{ psi} \quad (15)$$

where U_s is the slab-to-subbase friction factor,

Table 1. Prestress calculations.

Item	General Calculations	
	Slab 7 in Thick	Slab 8 in Thick
Slab length (ft)	250	350
Strand diameter (in)	0.6	0.6
Strand force (kips)	41	41
Strand spacing (in)	24	18
End of slab prestress (psi)	244	285
Prestress losses (psi)		
Shrinkage	6	6
Creep	4	6
Relaxation	20	23
Strand friction	39	62
Subbase friction	100	140
Total	169	237
Midslab prestress (psi)	75	48

Note: For the 8-in-thick design, actual tendon force selected is 44 kips. This results in an end of slab prestress of 306 psi and midslab prestress of 57 psi.

Table 2. Prestress loss computation coefficients.

Item	Magnitude
Tendon ultimate strength (psi)	270 000
Area, 0.6-in-diameter tendon (in^2)	0.217
Concrete creep coefficient	2.5
Concrete shrinkage strain (millionths)	150
Strand relaxation coefficient	
70 percent of ultimate stress	0.08
75 percent of ultimate stress	0.10
Wobble friction coefficient per foot	0.0014
Subbase friction factor	0.8
Modulus of elasticity of steel (million psi)	28
Modulus of elasticity of concrete (million psi)	5

and γ is the concrete unit weight (lb/ft^3).

Effective midslab prestress (f_p) is given by the following equation:

$$f_p = f_{pe} - f_t - f_s - f_{cr} - f_r - f_f \quad (16)$$

Example calculations for computing prestress losses and midslab prestress are given in Table 1. Coefficients and other values used for computations are listed in Table 2.

PROGRAM FORMULATION

Total flexural stress at the midslab edge is computed by using the following equation:

$$f_{T_{ijkl}} = f_{L_{ijkl}} + f_{C_{jkl}} - f_p - f_{W_{kl}} \quad (17)$$

where

$f_{T_{ijkl}}$ = total flexural stress for the ith axle group at the jth period of the day of kth month of lth year,
$f_{L_{ijkl}}$ = traffic load stress due to the ith axle group at the jth period of day of kth month of lth year,
$f_{C_{jkl}}$ = curling stress at the jth period of day of kth month of lth year,
f_p = effective prestress at midslab at the jth period of day of kth month of lth year, and
$f_{W_{kl}}$ = warping stress during kth month of lth year.

The anticipated number of repetitions (N_i) of stress of magnitude $f_{T_{ijkl}}$ is determined. Then, the allowable number of stress repetitions (NN_i) of magnitude $f_{T_{ijkl}}$ is calculated by using the fatigue model. Fatigue consumption (F_i) due to repeated stress applications of magnitude $f_{T_{ijkl}}$ is obtained as follows:

$$F_i = N_i/NN_i \quad (18)$$

Total fatigue consumption (F_{TOT}) during the design period is obtained by summing fatigue consumed by load repetitions for each stress level and is given by

$$F_{TOT} = \Sigma F_i \quad (19)$$

If total fatigue consumption at the end of the design period is less than 100 percent, the thickness obtained meets structural design criteria.

DESIGN EXAMPLE

The thickness design of a prestressed pavement for a heavily trafficked highway in central Illinois is presented. The high volume of heavy loads used is representative of traffic at locations where the concept of zero-maintenance pavements is applicable. The concept of zero maintenance implies use of a premium pavement at locations where higher first-cost is justified by a reduction in future costs due to repairs, user travel delays, and increased potential for accidents.

The design procedure may be used to determine the pavement thickness for any traffic mix. However, use of a thickness less than 6 in may not be practical, as space requirements for placing joint hardware such as anchors, seal holders, load-transfer devices, reinforcement, and positioning bars may not be available.

1. Project traffic data: The traffic distribution used was obtained from data gathered from field surveys and interviews by Darter and Barenberg (11). Average daily traffic (ADT) for the design period was selected as 6000 vehicles/day, the design life is 20 years, and the single-axle load distribution for the design lane during the design period is given in the table below:

Axle Load (kips)	No.
18-20	80 422
20-22	62 144
22-24	25 589
24-26	8 530
26-28	3 656
28-30	1 219
30-32	609
32-34	183

The tandem-axle load distribution for the design lane during the design period is as follows:

Axle Load (kips)	No.
38-40	29 244
40-42	11 576
42-44	4 874
44-46	3 656
46-48	1 828
48-50	1 219
50-52	1 219
52-54	609
54-56	183

2. The material properties are as follows: concrete modulus of elasticity, 5 million psi; concrete modulus of rupture, 700 psi; modulus of subbase reaction, 500 lb/in^3; diffusivity of

concrete, 5.24 in^2/h; and coefficient of thermal expansion of concrete, 0.000 005 in/in/°F.

3. The effective midslab prestress is 50 psi.

4. Warping restraint stress values are as follows: stress for a 7-in-thick slab is 190 psi, and stress for an 8-in-thick slab is 220 psi.

5. The results obtained by using the computer program are presented below:

Slab Thickness (in)	Edge Load Transfer Efficiency (%)	Fatigue Consumed (%)
7	0	2070
7	60	1
8	0	36

Based on above results, a 7-in-thick concrete pavement with a tied concrete shoulder or an 8-in-thick pavement without a tied concrete shoulder may be used.

SUMMARY

A computerized design procedure for prestressed concrete pavement is presented. The procedure is based on flexural stress analysis and prevention of bottom transverse cracking at the slab edge. Currently, only limited data are available to determine values for temperature cycle amplitude (θ_o) and warping restraint stress. Therefore, recommended design values may be used. The design procedure is simple to use and can be implemented immediately.

When prestressed and conventional pavements are compared for alternate designs, it is recommended that other factors in addition to first-costs be considered in the evaluation. These factors include a large reduction in the number of joints, which results in an improved riding surface and reduced number of lane closures for maintenance and repair.

ACKNOWLEDGMENT

Work was conducted by the Transportation Development Department of the Construction Technology Laboratories under the direction of Bert E. Colley. W.G. Corley, director, Engineering Development Division, reviewed the text of this paper and made valuable suggestions.

Bengt F. Friberg acted as a principal consultant and contributed to all phases of the study. His participation is gratefully acknowledged. T.F. McMahon and W. Kenis of FHWA provided technical coordination. Their cooperation and suggestions are gratefully acknowledged.

The opinions and findings expressed or implied in the paper are ours. They are not necessarily those of FHWA.

Discussions

Floyd J. Stanek

The comments presented in this discussion paper were formulated from information received while I served as technical monitor and coordinator for two studies of prestressed pavements sponsored by the Office of Research, FHWA. One study was a coordinated study by three state highway agencies to conduct an on-site inspection for the study, Performance of Prestressed Pavements in Four States. The representative members of this inspection team are as follows: Wade L. Gramling, Pennsylvania Department of Transportation (DOT); Gene Morris, Arizona DOT; and T. Paul Teng, Mississippi State Highway Department.

The other study was a follow-up research study of the Prestressed Pavement Demonstration Project, constructed in 1971-1972, near Dulles International Airport, Loudoun County, Virginia. This study was conducted by Bengt Friberg, one of the principal contributors to the original design and construction of this project. I served as monitor of this project for the FHWA Office of Research since 1972 and was closely associated with Friberg during the past 18 months for the completion of this study. A research report for each of these two studies is scheduled for future publication by FHWA.

For proper assessment, the subject paper, Prestressed Pavement Thickness Design, should be viewed in context of the following specific comments.

1. The paper deviates from the current practice of prestressing concrete pavements, which places the stressing tendons below midplane of the thickness of the pavement slab. This deviation will have a tremendous influence and effect on resistance to vehicle loads, fatigue properties, and other significant design advantages.

2. It is incorrect to use fatigue consumption as the design criteria based on bottom surface stresses at midslab only. The paper states that prestressing concrete increases the allowable stress in the flexural zone. It is statistically incorrect to use results from fatigue tests conducted on early-age, presumably 28-day-old, plain concrete for the design of prestressed pavements for a 20-year life. Prestressing improves material properties and the structural behavior of concrete pavements by preventing microcracking and maintaining internal stresses at advantageous levels. Fatigue properties of advanced-aged prestressed concrete are not currently available.

3. The design calculations for the one illustrative example presented are based on the assumption that only 50-psi prestress is available at midslab. Other designers and contributors to prestressed pavement technology claim midslab prestress of 200 psi or more can be maintained in slab lengths of 400 to 500 ft. For the two slab thicknesses of 7 and 8 in, the paper considers only slab lengths of 250 and 350 ft, respectively.

4. In the discussion of the temperature effects, the paper assumes a maximum daytime temperature gradient of 3°F. It is not clear as to how the design procedure evaluates and incorporates the corresponding time duration that this maximum gradient is imposed on the pavement. At any rate, previous contributors claim and substantiate that a temperature gradient of 3°F occurs in concrete pavements for only 1.73 percent of the time. This is less than a half-hour during each daily cycle. A comprehensive account of the time duration and corresponding temperature gradients through concrete pavements is presented by Swanberg (12). The paper also states that the accuracy of nighttime temperature is not as critical because these stresses are subtracted from load stresses. This is overconservative when fatigue consumption is used as the only design criteria.

5. The paper does not identify or characterize the serviceability requirements for a zero-maintenance pavement. But for the one prestressed zero-maintenance pavement presented, the paper recommends only a 7-in-thick slab tied to the shoulder or an 8-in-thick slab if not tied to the shoulder.

6. The vehicle load for the example presented is assumed to be 6000 ADT, whereas a traffic load of 21 000-27 000 ADT is assumed in an illustrative design of a zero-maintenance pavement presented elsewhere (11).

7. The paper states that the concept of zero maintenance is characterized primarily on economical and safety considerations on heavily traveled highways. But, the paper does not explain how these considerations are accounted for in the computerized program presented.

8. The paper's treatment of tendon relaxation behavior is not consistent with design aspects of prestressing pavement slabs or with the research results presented by Maguire, Sozen, and Siess (13). The inconsistencies are twofold, as stated herein and in comment 9. The paper assumes an initial prestressing force of only 70 percent of the strand's ultimate strength, whereas 80 percent is permitted by the American Concrete Institute (ACI) building code and has been used successfully by previous designers. This higher prestressing force increases the minimum prestress at midslab an additional 30-40 psi, permits longer slab lengths of 400 to 500 ft, and also becomes most advantageous for prestressing the gap slab as is done in some current designs.

9. The paper assumes that the relaxation coefficient for strands stressed to 70 percent of the ultimate strength remains constant along the length of the slab. In accordance with the values presented for the 7- and 8-in slabs in Tables 1 and 2, the stressing force at midslab due to strand frictional losses is only 59 and 55 percent of the ultimate strength, respectively. This will reduce the magnitude of the relaxation coefficient along the length of the slab substantially, perhaps by as much as 50 percent, at midslab.

10. A summary account of the performance, road tests, and measurements conducted on prestressed pavements constructed prior to 1976 in the United States, France, Holland, Switzerland, Belgium, Austria, and Germany is presented in a report by the Portland Cement Association (PCA) (14, pp. 68-103). Three of the five prestressed pavement demonstration projects constructed during the 1970s in four states with slab thickness of only 6 in are described in this report. An on-site inspection of these five projects was conducted during 1981 by the coordinated four-person team identified in the beginning of this discussion paper. The performance report by this inspection team is scheduled to be published in a future FHWA report.

11. In the results for the one design example presented, the paper states that a 7-in-thick concrete pavement may be used if tied to a concrete shoulder with a joint efficiency of 60 percent. In accordance with Equation 4a, a joint efficiency of 60 percent is equivalent to transferring 37.5 percent of the vehicle load to the shoulder. The paper does not explain how this partial transfer of the vehicle load is to be achieved or how this will affect the design and cost of the shoulder. Also, no accounting is presented as to how this tie with the shoulder will influence and effect the longitudinal stresses and movements of the slab due to temperature and moisture effects.

12. In the discussion of the example presented, the paper states that a slab thickness of less than 6 in may not be practical because of space requirements. No such problems have been reported for the prestressed pavements described in the PCA report (14) or in any of the highway prestressed pavements constructed with thicknesses of 6 in or less.

13. The paper's treatment of the frictional forces between pavement slab and subbase is not consistant with currently known technology as explained herein and in comment 14. In the design example presented, the paper does not state what friction-reducing medium was assumed between the pavement and the subbase. In Table 2, the paper shows a subbase friction factor of 0.8. This value is not correlated with the range of 0.3 to 0.8 for polyethylene sheets that could reduce to as low as 0.13 with special additives in accordance to the values presented in the PCA report (14, Table 14, pp. 164, 168).

14. In Table 1, the paper treats subbase friction as a prestress loss of 100 and 140 psi at midslab for the 7- and 8-in slabs, respectively. Previous contributors have shown and substantiated that the influence of the subbase friction can be either a positive or a negative effect, depending on whether the slab is expanding with warmer temperatures during the daytime (a positive effect) or is contracting with colder temperatures during the nighttime (a negative effect). For the values shown in Table 1, this could increase the midslab prestress an additional 200-240 psi for the daytime when the traffic volume is the highest. This phenomenon becomes most critical and important when the design criterion is based on fatigue consumption. In addition to others, this phenomenon has been reported and discussed in the literature (12;14, reference 87, p. 179; 15).

15. In the discussion of moisture effects, the paper acknowledges cyclic seasonal changes (7,8), but then apparently treats warping as a constant flexural stress with compressive stresses of 190 and 220 psi in the bottom of the 7- and 8-in slabs, respectively. The paper then states that the warping stresses cause a loss of support along the pavement edge, presumably to describe the effect in the lateral direction. The paper does not explain if and how this lateral effect influences or becomes combined with the corresponding flexural stresses in the longitudinal direction. All effects contributing to this combination must be time coordinated accurately when fatigue consumption is the only governing design criterion.

(Note: This discussion paper reflects my views and does not necessarily reflect the official views or position of FHWA.)

Bengt F. Friberg

The paper by Tayabji, Colley, and Nussbaum bases the determination of the thickness of prestressed pavements on a fatigue analysis for traffic loads for a 20-year period with an assumed strength of concrete given as a flexural strength of 700 psi. The paper includes a computer program for determining pavement thickness. Without more data from the computer program than are given, the results must be judged from the two examples presented: a 7-in-thick slab 250 ft long with edge load transfer in the transverse direction from the edge or an 8-in slab 350 ft long without edge load transfer.

These are relatively short and thick prestressed slabs compared with designs for recent prestressed U.S. highway projects that used greased posttensioned steel strands in extruded plastic tubing. The two design examples are believed to be the result of using a low limiting strand stress as well as high values of strand friction and subgrade friction. These and other conservative assumptions in fatigue stress analyses should be covered in other discussions.

It is desired to limit this discussion to the items of warping, length changes, and creep in concrete pavements, especially as they are evidenced in prestressed slabs where they appear to result in valuable and favorable distribution of prestress on the full-restrained sections. Such developments are

shown elsewhere (7), yet none of the applicable data have been included in the project reports. The reasons may be an unwillingness to accept that a pavement slab may grow, either seasonally or progressively. Evidence of growth is present in some slabs [the Rolla investigation (7)]. This information, along with similar information from other highway research, has been omitted from the reports.

Progressive growth of concrete pavements and the seasonal length change is shown in Figure 5, which was obtained in the pioneering work at the Bureau of Public Roads by Teller and Sutherland and furnished by E. C. Sutherland, and which covers the entire period that the pavement existed from 1930 to 1942. The seasonal length change would compensate for about 30°F of the annual temperature cycle.

The relatively high moisture content near the bottom is recognized as a permanent condition in pavement slabs. Figure 6 shows the moisture gradients from top to bottom of a 7-in road slab in Oregon for one year (16). Full saturation is 4.8 percent. The top of the slab dried out rapidly. No values were shown for the first inch of depth because its values varied from day to day or even hourly; however, at a 2-in depth, the slowly drying trend in the upper part is clear. The bottom 2 in show a continuing high moisture content at about 100 percent of saturation. These data are in agreement with observations by Carlson (17).

Tests of creep in concrete have been under way since before 1920 (18), including cylinders to 10-in diameter, different stress levels, and dry or moist storage for up to 30 years under load. The creep is measured in relation to unloaded control specimens

Figure 5. Progressive and seasonal length changes of 40-ft slabs.

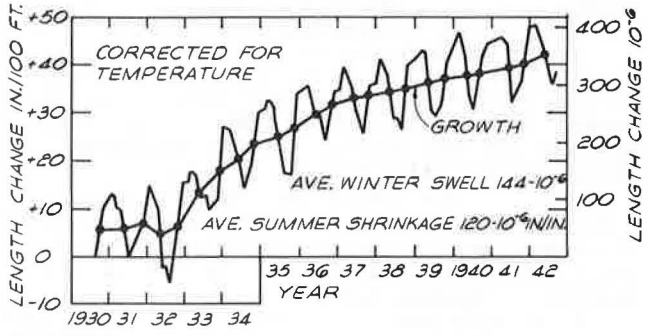

Figure 6. Moisture contents at 2 to 6 in depth in 7-in road slab in Oregon during the first year.

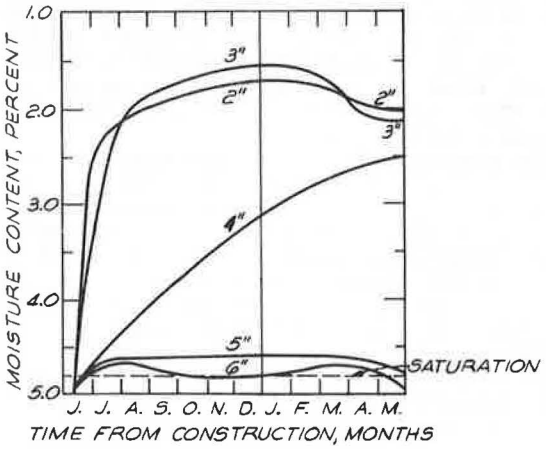

at the same storage. For storage at 100 percent relative humidity, cylinders showed swelling from 100×10^{-6} at 10 years to near 200×10^{-6} at 20 to 30 years of storage.

These and other creep data have been analyzed in accordance with theories by Ross, as published in the United States by Lorman (19), which give comprehensive coverage of the variables involved. A simple hyperbolic relation between creep strain (e_c) and time (t) in days under stress (f) by using a creep coefficient (M) defines the ultimate creep as strain per unit of stress, and a creep time constant of N days is used as follows:

$$e_c = [Mt/(N + t)]\, f \quad (20)$$

The so-called sustained modulus includes creep strain plus initial strain. By its use, stress information can be estimated at any time. Modulus of resistance is the term used elsewhere (7, Figure 11, Table 6).

Each value of the sustained modulus in the report by Friberg (7, Figure 11) is based on observations of six slabs, one dense and one air-entrained for prestress of 100, 300, and 500 psi. Good agreement and linearity can be seen. In each case, the sustained modulus at top is less than one-half of the sustained modulus at the bottom of the slabs. Lorman (19) shows creep coefficients increasing with decreasing moisture content and doubling as the relative humidity decreased from 100 to less than 70 percent. For the Rolla slabs, the creep coefficients at top and bottom were 0.5 and 0.2×10^{-6} in the 8-in slabs and 0.7 and 0.3×10^{-6}/psi in the 5.5-in slabs.

Because of the normal moisture gradients in pavements, differential shrinkage must be present as a common behavior in all slabs, including swelling at the bottom. Upward-warping deflections at the ends and edges is the result, so that the moment of the corresponding pavement weight redistribution may overcome the warping curvature that is unrestrained at the ends and that must be fully restrained in long slabs.

With a lower sustained modulus at the top than at the bottom, the flexural neutral axis can no longer be at middepth. Equal strains at the top and bottom section would mean unequal stress and lack of moment equilibrium. The simplest approximation is that the modulus varies linearly from top to bottom; the neutral axis can then be found for the trapezoidal stress areas.

In the paper, the neutral axis is assumed at middepth. A moisture gradient flexural restraint stress of 190 psi in 7-in slabs and 220 psi in 8-in slabs at bottom has been assumed, but the relation to the prestress, creep, and steel stress relaxation has not been explained. The restrained warping strain at the bottom of 150×10^{-6}, attributed to Friberg (7), is not clear. Nagataki shows that, for a warping unprestressed slab 284 in long and 10 in thick, strain differences between the end section and the fully restrained midsection of $+180 \times 10^{-6}$ at top and -130×10^{-6} at bottom, with the neutral axis well below middepth (8).

On the available data, compression stress at the bottom of 7-in slabs must be in excess of -480 and -550 psi in the 8-in slabs. The midlength effective prestress would be from 100 psi lower at night to 100 psi higher in daytime in the 7-in slab, with daily variations of ±140 psi in the 8-in slab.

If the lower sustained modulus that can naturally be expected at the surface had been recognized in the paper, an even more favorable effective prestress would have been computed. As indicated elsewhere (7, Figure 12), for 280-psi prestress on

the 8-in thickness, the stress at bottom is about -800 psi at two years, subject only to adjustment for steel stress relaxation.

Authors' Closure

We thank the discussants for their review of the paper. We believe there are many factors that influence concrete pavement performance that are not well understood and cannot be quantified. Also, because prestressed concrete pavements are thinner than conventional concrete pavements, deformation responses became more important. A significant amount of distress in concrete pavements is related to deformation. However, no practical criteria exist for including deformations in the design of concrete pavements. Therefore, the approach taken in formulating the design procedure has been to make assumptions that provide a reasonable margin of safety.

Design slab thickness is highly dependent on the number of repetitions and weight of the heaviest truck axles. We chose to provide a design example that uses heavy truck traffic. For less heavy traffic, a slab thickness of 6 in may be satisfactory. The design example should not be misinterpreted to mean all prestressed pavement should be 8 in thick or 7 in thick with tied shoulders. However, we believe that for zero-maintenance primary system highways, slab thickness should not be less than 6 in.

With regard to continued concrete growth with time, the information available seems to contradict Friberg's contention. Cracked and jointed concrete pavements do exhibit overall lengthening or growth. However, this growth is primarily due to the intrusion of incompressible material into cracks and joints. In addition, concrete slabs may exhibit growth if the concrete contains reactive aggregates. With regard to Figure 5, the concrete growth of about 350×10^{-6} in/in in the 40-ft slab that contained a midslab joint was measured by a micrometer at the slab surface. Thus, the data of Figure 5 represent slab growth of 350×10^{-6} in/in at the slab surface. We agree that concrete placed in a highly moist environment will exhibit growth. This growth, as discussed by Friberg, is only about 200×10^{-6} in/in for concrete cured continuously at 100 percent relative humidity from the time of casting up to a period of 20 years (18,20).

For a slab on grade, some growth due to moist conditions might be expected at the slab bottom. However, the slab surface would be expected to show drying shrinkage. Furthermore, this drying shrinkage at the slab surface is never fully recoverable under field conditions. This difference in moisture content between slab top and bottom is illustrated in Figure 6. Therefore, we cannot accept the application of the data of Figure 5 without serious reservations. In one of the 10-year reports on six experimental projects undertaken during the 1940s, Paxson, in describing the results of the Oregon studies, stated that "there is apparently no slab growth in the sense of a swell of the concrete due to physical or chemical change in the concrete itself. There is some evidence that shrinkage has been taking place" (21).

Similarly, results of the 10-year studies in other states indicate that, with few exceptions, all contraction joints experienced a gradual progressive increase in width during the first few years and very little increase in residual opening thereafter (22). In a recent National Cooperative Highway Research Program (NCHRP) report on joint-related distress in portland cement concrete (PCC) pavement, it is stated that the pavement lengthens due to infiltration and accumulation of incompressibles in joints and notes that "there is no permanent increase in the length of individual slabs" (23). Therefore, there is no clear consensus regarding continual growth of concrete in pavement slabs.

We do consider the effect of differential shrinkage on slab stresses. However, because of limited data, empirically derived values for warping restraint stresses are used.

The usual approach to thickness design of prestressed pavements is not to provide as much midslab prestress as possible. It is rather to provide a minimum level of prestress to ensure that any early cracks that may develop remain tightly closed. If a large midslab prestress is made available, then theoretically one could determine a design thickness of 4 to 5 in. However, balance must be maintained between theoretical calculations and practicability of construction. We do not object to use of higher prestressing levels but believe that higher prestress levels should be used to increase slab lengths or be used to provide an added factor of safety. Unless a satisfactory slab deformation response is assured, higher midslab prestress levels should not be used to result in significant slab thickness reductions.

With regard to comments by Stanek on pavement thickness, it is obvious to us that Stanek has overlooked the fact that the paper does recommend use of slab thicknesses of 6 in for prestressed concrete pavements. However, we do not recommend the use of thicknesses less than 6 in for reasons discussed in the paper and in this closure. Thus, the use of 6-in slab thickness for the demonstration projects is not contradictory to the paper. Responses to Stanek's specific comments follow.

1. For the four designs presented, tendons are placed about 0.5-1 in below slab middepth. Because of this steel location, the slab will retain better contact with the subgrade. This is an accepted practice and was followed on the Mississippi and Arizona demonstration projects (24,25).

2. We do not understand Stanek's comment on fatigue considerations. Because traffic loading on a pavement is of a repeated nature, the use of the fatigue considerations that we employed is general practice in pavement design.

3. As discussed previously, we do not have objections to use of higher midslab prestress. However, we do believe that prestress is primarily used to ensure that early non-load-related cracking is minimized.

As a point of interest, the calculated design midslab prestress for the Arizona demonstration project was 42 psi (25). The measured midslab prestress at the Mississippi demonstration project immediately after final prestressing was 60 psi for sections that incorporated two layers of polyethylene sheets under the slab (24).

4. The thickness design procedure does not use a linear temperature distribution for the slab as Stanek contends. As the discussion under temperature effect verifies, the design procedure uses a nonlinear temperature distribution. In addition, curling restraint stresses are computed for different periods of the day. This ensures a more realistic consideration of curling restraint stresses.

5. For the purpose of thickness design, the requirement for zero-maintenance pavements was that no load-associated cracking take place and that any early cracks remain tightly closed.

6. In the design procedure, ADT, axle load, and placement of axles are variables. The design example in the paper used the following vehicle parameters:

ADT (vehicles) = 6000,
Percentage of trucks = 11,
Percentage of directional distribution = 50,
Percentage of trucks in design lane = 100,
Mean axles per truck = 2.529, and
Percentage of trucks at edge = 20.

This results in 6 092 580 axles in the design lane in 20 years with 1 218 516 of these axles along the edge. This is a high level of truck axle loading and is equivalent to 22 000 ADT by using the vehicle parameters given elsewhere (11). As design engineers are aware, the number of axle loads at the edge is a more significant number than the ADT value.

7. The primary warrants for zero maintenance include reduced maintenance and user safety. These considerations are subjective and can only be established by each highway agency. However, the prestressed pavement design does ensure that a primary cause of maintenance activities, such as joint and crack-related distress, would be greatly minimized.

8. The paper does not put a limit of 70 percent of ultimate strength on the prestressing force in the tendons. The design process is iterative and use of tendon force of 70 percent of ultimate strength is made for the first trial. In fact, for the 8-in-thick design, although Table 1 shows trial calculations that use a 70 percent value, the final design value is 75 percent (26).

For the Arizona demonstration project, a 75 percent value was used. ACI Building Code 318-77 recommends use of a value of 70 percent after elastic shortening and anchorage slip losses have taken place but before time-dependent losses due to shrinkage, creep, and relaxation occur.

9. Stanek's comment on the relaxation coefficient for strands is not clear. As Table 1 indicates, losses due to steel relaxation are only 20 and 23 psi for the 7- and 8-in-thick pavements, respectively. Also, steel stresses at midslab immediately after prestressing are about 84 and 78 percent of that at slab ends for the 7- and 8-in-thick pavements, respectively. Steel stresses are not 59 and 55 percent as reported by Stanek. Reduction in computed prestress loss due to relaxation by using a nonuniform stress along the length of the tendons would be negligible.

10. As discussed previously, we do not recommend use of slab thicknesses less than 6 in. Thus, use of 6-in-thick prestressed slabs for low-volume and low-axle-weight loading is not contradictory to our presentation.

As a guide, the following thicknesses as related to traffic may be considered for pavements without a tied shoulder:

Truck Traffic Level	Slab Thickness (in)
Heavy	8
Medium	7
Light	6

11. At the pavement edge, load transfer is achieved by tieing the shoulder to the main slab by using deformed bars. The main slab and shoulder are placed in the same paving operation and prestressed at the same time. Thus, differential length changes would not occur.

12. Use of slab thickness less than 6 in is not considered practical because of difficulties that would be encountered during construction. In addition, use by medium to heavy truck traffic would result in significant levels of deformation-based distress. Also, Morris (27) of the Arizona DOT has reported that, from a construction standpoint, it is not desirable to have a prestressed pavement less than 6 in thick.

13. Stanek's view on the subbase friction reduction that can be achieved by using polyethylene sheets is not practical. Although laboratory tests on small specimens indicate lower values when using oil between two layers of polyethylene sheets, this method is not practical, is not used, and therefore cannot be recommended. Also, longer sections have differences in grade that result in larger frictional restraint values than those measured in the laboratory. The measured coefficient of subbase friction at the Mississippi demonstration project was about 0.6 when two sheets of polyethylene were used (24).

14. Prestress loss due to subbase friction is to account for frictional resistance encountered at the time of prestressing. It is not to account for the effect of decreasing slab temperature. Thus, once a stable slab-to-subbase interface condition is reached, decreasing temperature results in additional loss of effective prestress at midslab. Similarly, increasing temperatures result in compressive bottom frictional restraint stress.

The incorporation of frictional restraint stress due to the average slab temperature variation results in a more conservative design. Tensile frictional restraint stress during decreasing temperatures is of more significance to design than compressive frictional restraint stress during increasing temperature.

15. Cyclic seasonal changes do result in variations in warping restraint stresses. In fact, the computer program does consider monthly variations of warping restraint stresses. It should be noted, however, that during periods when the pavement surface is continually moist, warping restraint stresses may be lower due to smaller moisture differentials between the slab top and bottom.

With regard to the effect of loss of support due to warping, Equations 1 and 3 were developed by using a finite-element computer program that includes loss of support along the pavement edge. The net effect of loss of support is to increase traffic load associated stresses in the longitudinal direction.

REFERENCES

1. S.D. Tayabji, B.E. Colley, and P.J. Nussbaum. Prestressed Pavement Thickness Design. FHWA, June 1981.
2. S.D. Tayabji and B.E. Colley. Analysis of Jointed Concrete Pavements. FHWA, Oct. 1981.
3. D.K. Emery, Jr. Paved Shoulder Encroachment and Transverse Lane Displacement for Design Trucks on Rural Freeways. Paper presented to Committee on Shoulder Design, Transportation Research Board, Washington, DC, Jan. 1974.
4. J. Thomlinson. Temperature Variations and Consequent Stresses Produced by Daily and Seasonal Temperature Cycles in Concrete Slabs. Concrete and Construction Engineering, June 1940.
5. S.G. Bergstrom. Temperature Stresses in Concrete Pavements. Swedish Cement and Concrete Research Institute, Royal Institute of Technology, Stockholm, 1950.
6. The AASHO Road Test: Report 5, Pavement Research. TRB, Special Rept. 61E, 1962.
7. B.F. Friberg. Investigations of Prestressed

Concrete for Pavements. HRB, Bull. 332, 1962, pp. 40-94.
8. S. Nagataki. Shrinkage and Shrinkage Restraints in Concrete Pavements. Journal of the Structural Division, ASCE, July 1970.
9. J.W. Murdock. A Critical Review of Research on Fatigue of Plain Concrete. Engineering Experiment Station, Univ. of Illinois, Urbana, Bull. 475, 1965.
10. Thickness Design for Concrete Pavements. Portland Cement Association, Skokie, IL, 1966.
11. M.I. Darter and E.J. Barenberg. Design of Zero Maintenance Plain Jointed Concrete Pavement: Vol. II, Design Manual. FHWA, Rept. FHWA-RD-77-112, June 1977.
12. J.H. Swanberg. Temperature Variation in a Concrete Pavement and the Underlying Subgrade. HRB, Proc., Vol. 25, 1945, pp. 69-180.
13. B.M. Maguire, M.A. Sozen, and C.P. Siess. A Study of Stress Relaxation in Prestressing Reinforcement. Journal of the Portland Cement Association, April 1964, pp. 13-57.
14. A.N. Hanna, P.J. Nussbaum, T. Arriyavat, J. Tseng, and B.F. Friberg; Portland Cement Association. Technological Review of Prestressed Pavements. FHWA, Rept. FHWA-RD-77-8, Dec. 1976.
15. E.F. Kelley. Structural Design of Concrete Pavement. Journal of the American Concrete Institute, Vol. 35, Supplement, Sept. 1939.
16. G.S. Paxson. Investigational Concrete Pavement in Oregon. HRB, Res. Rept. 3B, 1945, pp. 77-89.
17. R.W. Carlson. Drying Shrinkage of Large Concrete Members. Journal of the American Concrete Institute, Jan.-Feb. 1937, pp. 327-336.
18. G.E. Troxell, J.M. Raphael, and R.E. Davis. Long-Time Creep and Shrinkage Tests of Plain and Reinforced Concrete. Proc., ASTM, Vol. 58, 1958, pp. 1101-1120.
19. W.R. Lorman. The Theory of Concrete Creep. Proc., ASTM, Vol. 40, 1940, pp. 1082-1102.
20. A.M. Neville. Properties of Concrete. Pitman Publishing, Ltd., London, 1981.
21. G.S. Paxson. Report on Experimental Project in Oregon. HRB, Res. Rept. 17B, 1956, pp. 151-155.
22. E.C. Sutherland. Analysis of Data from State Reports. HRB, Res. Rept. 17B, 1965, pp. 1-11.
23. Joint-Related Distress in PCC Pavement: Cause, Prevention, and Rehabilitation. NCHRP, Synthesis of Highway Practice 56, 1979.
24. G.E. Albritton. Prestressed Concrete Highway Pavement: Performance During Construction. Paper presented at 57th Annual Meeting, Transportation Research Board, Washington, DC, Jan. 1978.
25. G.R. Morris and H.C. Emery. The Design and Construction of Arizona's Prestressed Concrete Pavement. Research Section, Highway Division, Arizona Department of Transportation, Phoenix, Jan. 1978.
26. P.J. Nussbaum, S.D. Tayabji, and A.T. Ciolko. Prestressed Pavement Joint Design. FHWA, June 1981.
27. G.R. Morris. Full-Depth, Full-Width Designs and Prestressed Concrete Pave the Way for Arizona's Highways. Civil Engineering, ASCE, March 1978.

Publication of this paper sponsored by Committee on Rigid Pavement Design.

Comparison of Solutions for Stresses in Plain Jointed Portland Cement Concrete Pavements

D. R. MacLEOD AND C. L. MONISMITH

A number of existing models to compute the stresses in plain jointed portland cement concrete (PCC) pavements due to traffic loads are examined, and those that show the most promise are recommended. Solutions examined include (a) plate on dense-liquid subgrades, closed form and finite elements; (b) plate on elastic solid, closed form and finite element; and (c) layered elastic system, closed form and finite element (two-dimensional and three-dimensional representations). Although the three-dimensional finite-element analysis for the layered elastic solid is probably the most representative of the methods examined, the associated computer costs preclude its use on a routine basis at this time. The study does show that a two-dimensional finite-element analysis for the same representation is suitable for determining load-associated stresses in plain jointed PCC pavements. Changes in the engineering properties of materials, climate variations, and loading conditions can be accommodated. The maximum tensile stress—the controlling factor in the fatigue life of PCC pavements—occurs near the edge of the PCC at the midslab position. A finite-element analysis, which allows for the consideration of the strengths of the cement-stabilized layer (not accounted for in a dense-liquid subgrade type of analysis), has demonstrated that the stiffness of the cement-stabilized layer has an important effect on the fatigue life of PCC pavements. This analysis has indicated that different cracking-behavior patterns can be identified with different stabilized layer stiffnesses. A detailed traffic analysis, with allowances for thermal stresses and material variabilities, has indicated that there is a common fatigue relation for PCC pavements when the failure criteria $N_f = 225\,000\,(MR/\sigma)^4$ is used.

It has long been recognized that cracking in portland cement concrete (PCC) pavements cannot be related to traffic alone, but such factors as climate, pavement material stiffnesses, strengths, and thicknesses are significant in establishing pavement behavior as well. To date, mechanistic models have not been able to deal satisfactorily with these factors. This paper examines some of the existing models that have been used to analyze the development of load-associated cracking in plain jointed PCC pavements. Based on these analyses, those representations that have promise are recommended for use, recognizing that a satisfactory predictive model for PCC pavement cracking should

1. Predict the location, type, and severity of distress;
2. Be adaptable to various climatic conditions;
3. Allow for changes in the engineering properties of materials (in particular, the model should realistically reflect the influence of various stabilized subbases on performance);
4. Allow for changes in loading conditions (this